# Dynamical inhomogeneity of liquid Te near the melting temperature proved by the inelastic x-ray scattering measurements

**Y Kajihara[1], M Inui[1], S Hosokawa[2], K Matsuda[3] and A Q R Baron[4]**

[1] Graduate School of Integrated Arts and Sciences, Hiroshima University, Higashi-Hiroshima, 739-8521, Japan
[2] Center for Materials Research using Third-Generation Synchrotron Radiation Facilities, Hiroshima Institute of Technology, Hiroshima, 731-5193, Japan
[3] Graduate School of Engineering, Kyoto University, Kyoto, 606-8501, Japan
[4] SPring-8/RIKEN, 1-1-1 Kouto, Sayo-cho, Sayo-gun, Hyogo, 679-5148, Japan

E-mail: `kajihara@hiroshima-u.ac.jp`

**Abstract.** High-frequency dynamics of liquid Te near the melting temperature has been investigated by the inelastic x-ray scattering measurements. Dynamic structure factors $S(Q, E)$ are obtained at 500, 650 and 800 °C. Acoustic excitation is ascertained at each temperature: its $Q$- dependent phase velocity $v(Q)$ switches from high-frequency value $v_{\mathrm{IXS}}$ to the ultrasonic value $v_s$ at some momentum transfer $(Q = Q_{\mathrm{trans}})$. With decreasing temperature, both the positiveness $(\equiv (v_{\mathrm{IXS}} - v_s)/v_s)$ and the effective length $(\equiv 2\pi/Q_{\mathrm{trans}})$ increase, which means that the structural relaxation in liquid Te changes much in this temperature region. With the aid of the thermodynamic formulation, we show that it should be an evidence of the *dynamical* inhomogeneity: it can be much enhanced by the M-NM transition which exists in the supercooled region. The *dynamical* inhomogeneity may be induced by the *second* critical phenomena which is similar to liquid water.

## 1. Introduction

Liquid Te has been known a very mysterious material and has been fascinating many researchers for over half century. Te is a typical semiconductor in the solid phase, but it shows metallic nature in the liquid phase [1]. This change in the electrical property is believed to be closely related to the structural change in Te [2]. In the solid phase, Te consists of two-fold coordinated covalent-bonded chains and a stable crystal at the ambient conditions has a trigonal form which is commonly seen in solid selenium, the same chalcogen element. But on melting, the coordination number in liquid Te becomes around three [3], and the density becomes slightly higher than in the solid phase. The most remarkable features of liquid Te are thermodynamic anomalies. The temperature dependence of the density shows a maximum [4] at around melting temperature $(T_m \simeq 450°\mathrm{C})$ and with increasing temperature, the heat capacity *decreases* [5] and the ultrasonic sound velocity *increases* [6, 7] near the melting temperature. These features are anomalous compared to normal liquids, however, it is very similar to liquid water [8] and liquid Si, which are sometimes called an *anomalous*

*liquid*. Water exhibits a density maximum at 277 K and the sound velocity of water *increases* with increasing temperature around the melting temperature.

To explain the thermodynamic anomalies in liquid Te, Tsuchiya and Seymour proposed an inhomogeneous structure model over twenty years ago [9]. They assumed that there exists inhomogeneity which consists of metallic and nonmetallic mesoscopic domains in liquid Te. This inhomogeneous structure model was consistent with the previous two-species model [10, 11] and inhomogeneous *transport* model [12] which had been introduced to account for the *electronic* properties (electrical conductivity , Hall coefficient and nuclear magnetic resonance Knight shift) in liquid Te. The inhomogeneous structure model partially explained both the thermodynamic anomalies and the electronic properties reasonably, but there seem to remain two unsolved problems. The first one is that no one have succeeded in the direct observation of this inhomogeneity. We know that some researchers tried to conduct small-angle x-ray and neutron scattering measurements but they observed almost no scattering intensities, resulting in no report of them. The second problem is that the model did not explain why there is inhomogeneity in liquid Te. In the model, the inhomogeneity may have been introduced only as a phenomenological input parameter.

Because of these two unsolved problems, the inhomogeneous structure model has not been widely accepted and liquid Te remains to be an *anomalous liquid*. In order to tackle with this anomalous liquid Te, we have carried out inelastic x-ray scattering (IXS) measurements at SPring-8 in Japan. As already mentioned, liquid Te has been fascinating to many researchers and up-to-date results on the local structure in liquid Te was reported [13]. About the dynamical structure in liquid Te, quasielastic and inelastic neutron scattering (INS) measurements were carried out to investigate the temperature dependence of the diffusive character and the vibrational density of states [14, 15, 16]. Recently the dispersion of the acoustic mode at low $Q$ were reported by INS [17] and IXS [18] measurements for liquid Te. However these measurements did not clarify the temperature dependence of the dispersion relation. In the previous paper [19], we reported the precise temperature dependence of the dispersion relation for the acoustic mode in liquid Te. In this paper, we report details of the experimental results and propose a concept to explain not only IXS results but also the unsolved problems mentioned above.

## 2. Experiment

The experiments were carried out at the high-resolution inelastic scattering beamline BL35XU of SPring-8 in Japan [20]. The energy of incident x-ray is highly monochromatized to 21.748 keV by Si(11 11 11) back scattering monochrometer, the scattered x-ray was analyzed by 12 Si crystal analyzers and the final energy resolution of the measurements was 1.5-1.8 meV HWHM.

Liquid Te sample with a thickness of 290 $\mu$m was contained in a thin-walled single-crystalline sapphire cell [21]. The cell was located in a vessel [22] equipped with single-crystal Si windows capable of covering scattering angle between $0°$ and $25°$. The vessel was filled with about 2bar He gas of 99.9999% purity in order to reduce evaporation of liquid Te. The IXS spectra were measured and the momentum transfer ranges between 1.3 and 43 nm$^{-1}$ at 500 and 800 °C and between 1.3 and 27 nm$^{-1}$ at 650 °C. Empty cell and and polymethyl methacrylate (PMMA) measurements were separately carried out for background corrections and resolution function determination, respectively.
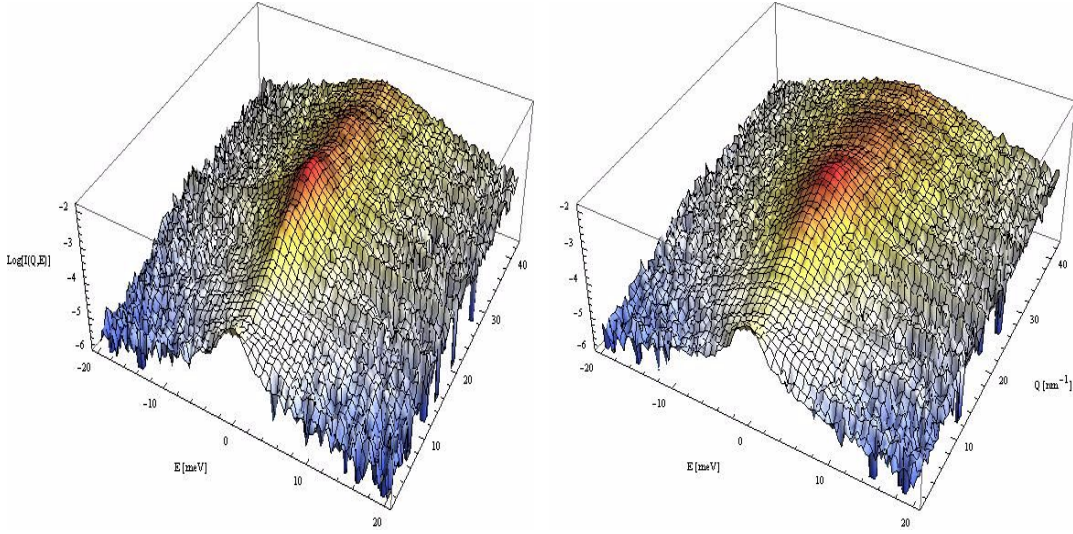
**Figure 1.** (Colour online) IXS spectra $I(Q, E)$ at 500 (left) and 800 °C(right).

## 3. Results

Figure 1 show the measured IXS spectra $I(Q, E)$ at 500 and 800 °C. Background scattering intensity from the cell is subtracted and the spectra are modified with the $Q$ dependence of the atomic form factor. $I(Q, E = 0)$ in both temperatures show peaks at around $Q = 20$ and 32 nm$^{-1}$ where the static structure factors $S(Q)$ (see figure 2) exhibit maxima. With increasing temperature, these peaks become broader in both $Q$- and $E$- directions because the randomness of the atomic position become larger in both space and time. We evaluate the reliability of the present data by comparing $I(Q)$, the integration of $I(Q, E)$ with respect to $E$ as equation (1), with $S(Q)$.

$$I(Q) = \int I(Q, E)dE. \tag{1}$$

In figure 2 (a), open circles indicate $I(Q)$ at 500 °C. It almost coincides with $S(Q)$ denoted by a solid curve, which is obtained from neutron diffraction measurements [23]. In figure 2(b), open symbols indicate $I(Q)$ in small $Q$ region at all temperatures. Closed symbols are $S(0)$ calculated from the pressure $(P)$ variation of the density $(\rho)$ [24] by the following equation:

$$S(0) = \frac{\rho}{m}k_B T \left[ \frac{1}{\rho} \left( \frac{\partial \rho}{\partial P} \right)_T \right], \tag{2}$$

where $k_B$ is the Boltzmann constant, $m$ is atomic mass of Te and $T$ is the temperature. The consistency between $I(Q)$ from the present IXS and $S(0)$ from the density measurements is very well at all temperatures. There is no divergence in small $Q$ regions, which is consistent with the previous unpublished studies on small-angle scattering, and it can be concluded that there is only a small *density* inhomogeneity in liquid Te at these temperatures.

There seem no distinct side peaks $(E \neq 0)$ or the mode in $I(Q, E)$ spectra in figure 1, but we can surely ascertain the acoustic mode when we analyze the spectra
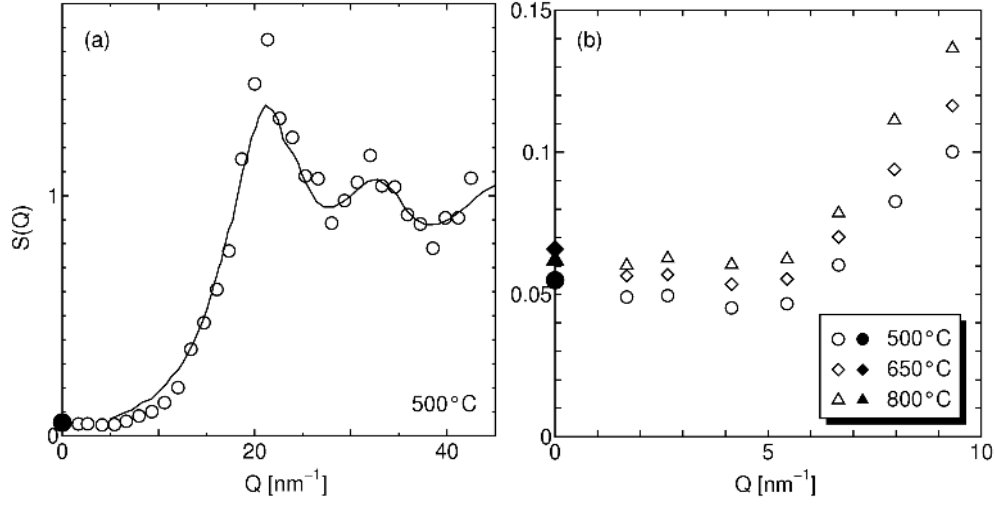
**Figure 2.** Open symbols indicate $I(Q)$ (a) at full-$Q$ region at 500 °C and (b) small $Q$ region at all temperatures. Solid curve and closed symbols are the static structure factors $S(Q)$ from ND [23] and the density measurements [24]. Circles, squares and triangles correspond to the data at 500, 650 and 800 °C, respectively.

by a damped harmonic oscillator (DHO) model. In this model, the quasi-elastic line of a simple Lorentzian is assumed, and the inelastic mode is expressed by DHO given as,

$$\frac{I(Q,E)}{I(Q)} = \int \frac{S(Q,E)}{S(Q)} R(R, E - E') dE'$$

$$\left( \frac{S(Q,E)}{S(Q)} \right) = \left( \frac{E/k_B T}{1 - e^{-E/k_B T}} \right) \times$$

$$\left[ \frac{A_L}{\pi \Gamma_L} \frac{\Gamma_L}{E^2 + \Gamma_L^2} + \frac{A_{\mathrm{DHO}}}{\pi \hbar / k_B T} \frac{4 \Gamma_{\mathrm{DHO}} \sqrt{E_{\mathrm{DHO}}^2 - \Gamma_{\mathrm{DHO}}^2}}{(E^2 - E_{\mathrm{DHO}}^2)^2 + 4 \Gamma_{\mathrm{DHO}}^2 E^2} \right]. \tag{3}$$

Here $A_L$ and $\Gamma_L$ are the amplitude and the width of the central Lorentzian and $A_{\mathrm{DHO}}$, $\Gamma_{\mathrm{DHO}}$ and $E_{\mathrm{DHO}}$ are the amplitude, width and energy of DHO, respectively. $R(E)$ represents the resolution function deduced from the PMMA measurements. The parameters in the above model were optimized by the non-linear least square method. The most important parameter in this model is $E_{\mathrm{DHO}}(Q)$ or the dispersion curve of the acoustic mode, which is indicated by open circles in figure 3 (a) 500, (b) 650 and (c) 800 °C. They disperse almost linearly in the small $Q$ region, which means that they are the acoustic modes, but the dispersion is much faster than that of the ultrasonic sound indicated by the dashed lines. They show dips at around $Q = 20$ and $32$ nm$^{-1}$ where the $S(Q)$ have maxima or the pseudo-zone boundaries. These features prove that they are exactly the phonon-like modes. In the high $Q$ region, they approach to the dotted lines which are calculated from the thermal velocities $v_{th} = \sqrt{3k_B T / 2m}$, which means that the modes represent only self-correlations in these high-$Q$ regions.

We deduce the phase velocity of this phonon-like mode by $v(Q) \equiv E_{\mathrm{DHO}}(Q)/Q$ and show the value in the small $Q$ region by open circles in figure 4 at (a) 500, (b) 650 and (c) 800 °C. We define $v_{\mathrm{IXS}}$ by $v(Q)$ value in its flat region and the *positiveness* by the normalized difference between $v_{\mathrm{IXS}}$ and $v_s$, $(v_{\mathrm{IXS}} - v_s)/v_s$. This positiveness
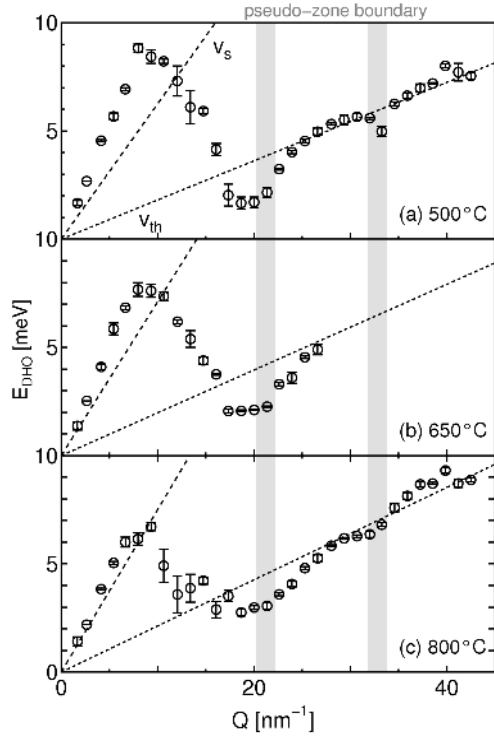
**Figure 3.** Dispersion curves at (a) 500, (b) 650 and (c) 800 °C. Open circles are from the present IXS experiments and dashed lines and dotted lines are the ones from the ultrasonic sound velocities [7] and thermal velocities of atoms.

changes much against the temperature: from higher temperature side, it is about 20 % at 800 °C, which is normal value for ordinary liquids. It decreases with increasing temperature, and reaches about 70 % at 500 °C, which is much large compared to the ordinary liquids. We also define $Q_{\text{trans}}$ where $v(Q)$ approach to $v_s$ in smaller $Q$ region (hatched area). $Q_{\text{trans}}$ is about 2.5nm$^{-1}$ at 800 °C, shifts to smaller value with decreasing temperature and seems to become smaller than the smallest $Q$ (1.5nm$^{-1}$) in the present measurement at 500 °C.

Temperature dependences of these parameters are plotted in figure 5. The M-NM transition is believed to exist in the supercooled region and its transition temperature can be estimated to be around 300-350 °C[25, 26] Sound velocities deduced by other authors are also plotted: open symbols denote the dynamical sound velocities obtained from the present IXS (circles), the previous IXS (triangles) [18] and the inelastic neutron scattering (INS) (crosses) [17]. The consistency among these dynamical velocities is good. Dashed line is the adiabatic value measured directly from the ultrasonic method [7]. With decreasing temperature, $v_{\text{IXS}}$ normally *increases* while $v_s$ anomalously *decreases*. Thus, the positiveness substantially increases with decreasing temperature. The effective length, which is defined from $Q_{\text{trans}}$ by $l_{\text{eff}} \equiv 2\pi/Q_{\text{trans}}$ and denoted by closed circles, also increases in the mesoscopic order ($\sim$nm) with decreasing temperature. The present results hint that there exist a mesoscopic structural relaxation and it may be a direct evidence of the *dynamical* inhomogeneity
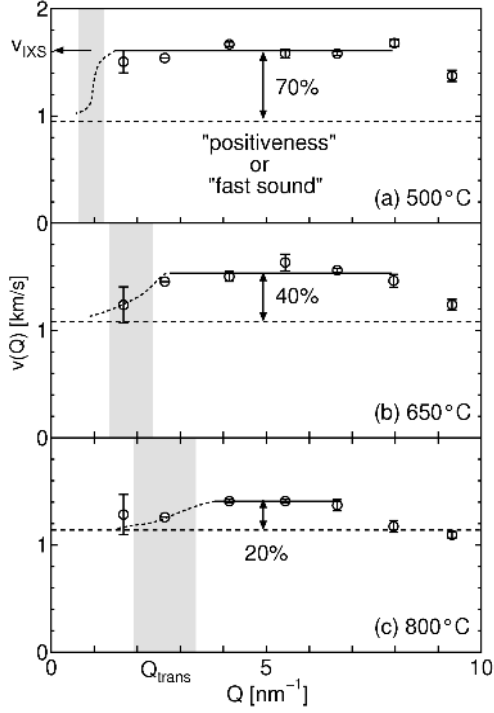
**Figure 4.** Open circles indicate the Q-dependencies of the phase velocity $v(Q)$ at (a) 500, (b) 650 and (c) 800°C. $v(Q)$ change from the high-frequency value $v_{\text{IXS}}$ to the ultrasonic one $v_s$ in $Q_{\text{trans}}$ region (hatched area). We define the *positiveness* by the normalized difference between $v_{\text{IXS}}$ and $v_s$.

in liquid Te. In the next section, we will describe our interpretation and show what is the entity of the *dynamical* inhomogeneity and its relation with the M-NM transition.

## 4. Discussion

The $Q$ dependence of the dynamical sound velocity shown in figure 4 may be regarded as the hydrodynamic visco-elastic transition commonly observed in many liquids. However the opposite temperature dependence between IXS and ultraonic sound velocities let us consider it more carefully. The present observation clearly show that the anomalous slowing down of the ultrasonic sound with decreasing temperature is not related to the structural relaxation in the frequency region probed by the present IXS but to much slower one. Now we discuss it from the view-point of thermodynamics. In fluid systems, the sound velocity $v_s$ is related to the adiabatic compressibility $\beta_S$,

$$\frac{1}{\rho v_s^2} = \beta_S = -\frac{1}{V}\left(\frac{\partial V}{\partial P}\right)_S \tag{4}$$

where $V$ is the molar volume of the sample and $S$ is the entropy of the system. When the system has an internal degree of freedom $x$, which generates an inhomogeneity, this equation should be modified to,

$$\frac{1}{\rho v_s^2} = -\frac{1}{V}\left(\frac{\partial V}{\partial P}\right)_{S,x} - \frac{1}{V}\left(\frac{\partial V}{\partial x}\right)_P \left(\frac{\partial x}{\partial P}\right)_S. \tag{5}$$
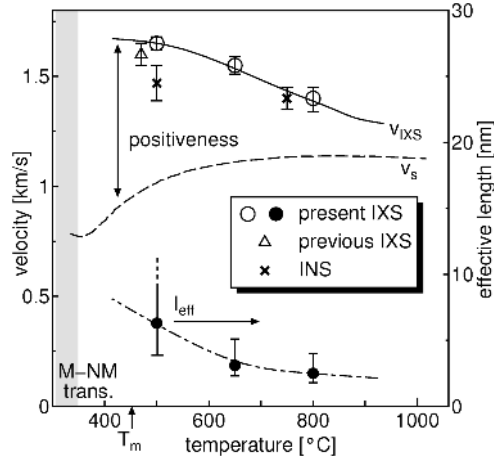
**Figure 5.** Sound velocities obtained from various methods and effective length defined by the present IXS. Open symbols are the dynamical values deduced from $S(Q,E)$ of the present IXS (circles), the previous IXS [18] (triangles) and INS [17] (crosses) measurements. A dashed line is the adiabatic value by the ultrasonic sound measurement [7]. A solid line and a dot-dashed line are guides for the eyes. The M-NM transition temperature is estimated to be around 300-350 °C [26, 25] in the supercooled region.

.

Then excess compressibility $\beta_r \equiv -\frac{1}{V}\left(\frac{\partial V}{\partial x}\right)_P \left(\frac{\partial x}{\partial P}\right)_S > 0$ arises and it slows down $v_s$. When this inhomogeneity has a *dynamical* nature, which means that the inhomogeneity fluctuates with its characteristic time constant, the situation is slightly changed. In this case, if the frequency of the sound wave is high enough compared to the characteristic frequency of the fluctuations, the high-frequency compressibility $\beta_{HF} \equiv -\frac{1}{V}\left(\frac{\partial V}{\partial P}\right)_{S,x} > 0$ is observed. These equations are established in the theory of acoustic properties [27], and here we are extending this formulation to the present IXS region. We assume that IXS measures this high-frequency compressibility $\beta_{HF}$ [?], and the difference between $v_{IXS}$ and $v_s$ is the excess compressibility itself as,

$$v_{IXS} \simeq v_{HF} \equiv \frac{1}{\sqrt{\rho\beta_{HF}}} = \frac{1}{\sqrt{\rho(\beta_S - \beta_r)}}, v_s = \frac{1}{\sqrt{\rho\beta_S}}. \tag{6}$$

Specific formulation of $\beta_r$ can be deduced by assuming a simple two-state model (see figure 6) [29]. If the two states are in equilibrium with a energy difference $\Delta G$, an equilibrium constant $K$ can be written as,

$$K = \frac{x}{1-x} = \exp(-\frac{\Delta G}{k_B T}). \tag{7}$$

Thus, excess compressibility is expressed by

$$\beta_r = \frac{x(1-x)}{k_B T}\left(\frac{|\Delta V|}{V}\right)\left(\frac{\partial \Delta G}{\partial P}\right)_S \tag{8}$$

with $\Delta V$ is molar volume difference between the two state. When the energy difference is only the density difference $\Delta G = |-p\Delta V|$ as shown in figure 6(a), excess compressibility is

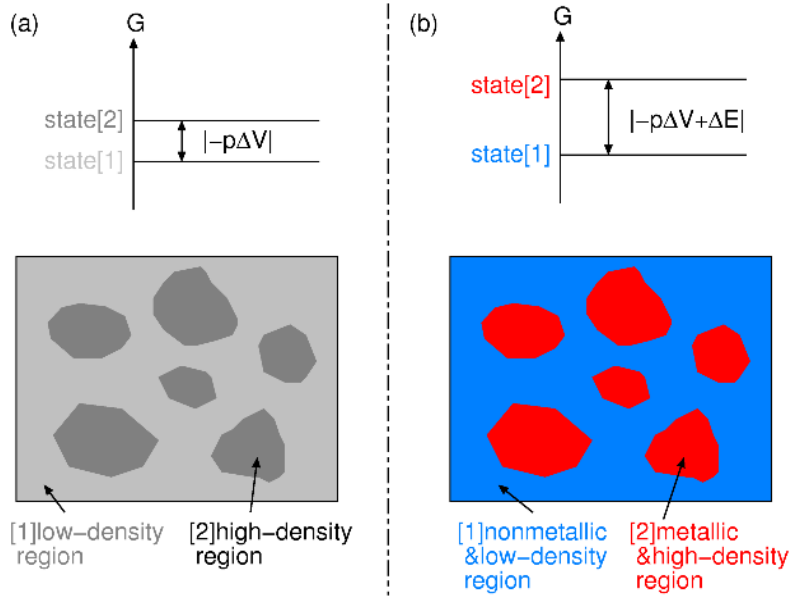$$\beta_r = \frac{x(1-x)}{k_B T}\left(\frac{|\Delta V|}{V}\right)|\Delta V|. \tag{9}$$

**Figure 6.** (Colour online) 2-state model and its schematic diagram of inhomogeneity in fluid system. (a) pure density inhomogeneity and (b) density inhomogeneity with metallic nature difference.

| temperature [ °C] | 500 | 650 | 800 |
|---|---|---|---|
| $x$ | 0.88 | 0.97 | 0.99 |
| $|\Delta V|/V$ | 0.15 | 0.22 | 0.27 |
| $\beta_r$ from IXS [/TPa] | 10.3 | 7.0 | 4.6 |
| $\beta_r$ from volume [/TPa] | 0.7 | 0.4 | 0.1 |

**Table 1.** $\beta_r$ estimated from two methods. See details in the text.

$\beta_r$ is proportional to the square of the volume inhomogeneity $|\Delta V|$. This is the normal slowing-down phenomena which is commonly observed in the density fluctuations near the liquid-gas critical point. In ordinary fluids, $\beta_r$ shows 3D-Ising class divergence with approaching to the critical point [30]. But when $\Delta G$ has another contribution of the internal energy difference, $\Delta G = |-p\Delta V + \Delta E|$ as shown in figure 6(b), where we suppose that $\Delta E$ should be large because the energy difference between metallic and nonmetallic states is expected to be $10^{-1}$ eV order while $|-p\Delta V| \sim 10^{-5}$ eV, it becomes,

$$\beta_r = \frac{x(1-x)}{k_B T} \left( \frac{|\Delta V|}{V} \right) \left( |\Delta V| + \left( \frac{\partial \Delta E}{\partial P} \right)_S \right). \tag{10}$$

$\beta_r$ is enhanced by the pressure variation of $\Delta E$.

We apply this formulation to the present result. From equation (6) and the observed positiveness, $\beta_r$ can be calculated, while $\beta_r$ is also estimated from equation (9) with using the value $x$ [12] and $|\Delta V|$ [9] from the literature. The results are summarized in table 1. $\beta_r$ estimated from the pure density inhomogeneity is much smaller than that obtained from the present IXS measurement. Thus, we need to

consider other contribution. The enhancement factor $(= |\Delta V| + \left(\frac{\partial \Delta E}{\partial P}\right)_S \sim \left(\frac{\partial \Delta E}{\partial P}\right)_S)$ should be very large one which is more than 10, using equation (10).

As is shown above, it may be difficult to estimate exact $\left(\frac{\partial \Delta E}{\partial P}\right)_S$ in liquid Te from the available data. However the experimental results of another fluid accompanying the M-NM transition would help to validate the present thermodynamic consideration. In supercritical fluid Hg, the M-NM transition occurs at the density of 9 g/cm$^{-3}$ near the liquid-gas critical point [31]. Thus fluctuations are induced by the liquid-gas critical phenomena in the transition region [32]. Ishikawa et al. [33] carried out IXS measurements of supercritical fluid Hg and reported that the excitation energy of the acoustic mode disperses three times faster than the adiabatic sound velocity at around the M-NM transition. This is crucial information that the enhancement factor is inferred to be very large. Similarly the ultrasonic absorption measurements for supercritical fluid Hg shows that the absorption coefficient exhibits double peaks at 9 g/cm$^{-3}$ in the M-NM transition and at the critical density (5.8g/cm$^3$) [34]. Since the absorption coefficient of ultrasonic waves is proportional to $\beta_r$ [34], these results from the ultrasonic measurements hint that the enhancement factor becomes large at the M-NM transition while the effect of the density fluctuations become dominant near the liquid-gas critical region. From the results of liquid Te and fluid Hg, we can speculate that the enhancement factor becomes very large with approaching the M-NM transition region. The large enhancement factor implies that the M-NM transition is essentially first order in these systems because $\Delta E$ and its derivative with respect to $P$ must show step-wise behaviour at the M-NM transition point. We can also conclude that it is the origin of the first problem of liquid Te which is mentioned in the introduction section, that there is only small *density* inhomogeneity but there exists large *dynamical* inhomogeneity near the melting temperature in liquid Te.

In order to solve the second problem why there is inhomogeneity in liquid Te, it may be effective to pay attention to the similarity between liquid Te and water. In water system, a *second* critical concept has been suggested to explain the complexity of the liquid: in the supercooled region, there exist two liquid states, high-density and low-density liquids, and the first-order transition between these two phases has a *second* critical point [35, 36] (of course, the first one is liquid-gas critical point). In this concept, the structure and thermodynamics of water at ambient conditions are affected by the *second* critical fluctuations. By simply introducing this concept to the liquid Te, the second problem can be solved: inhomogeneity of liquid Te is induced by the *second* critical fluctuations as shown in figure 7, where liquid Te has two phases which are metallic high-density and non-metallic low-density ones. The first-order transition between these two phases exists in the supercooled region and the second critical point exists. Thus, this phase transition at ambient pressure, which is expected to be under the critical pressure, should become second order and will exhibit the continuous change in the supercooled region. In fact, with decreasing temperature, continuous changes were observed in the structure down to 300 °C [25] and the electrical conductivity down to 370 °C [26] in the supercooled liquid Te.

## 5. Conclusion

We have observed the temperature dependence of dynamical sound velocity in liquid Te by IXS technique and found that with decreasing temperature, it increases while the ultrasonic sound velocity decreases. Thus the positiveness exhibits a large value of 70 % near the melting temperature, compared to 10-20 % reported in many liquid metals.
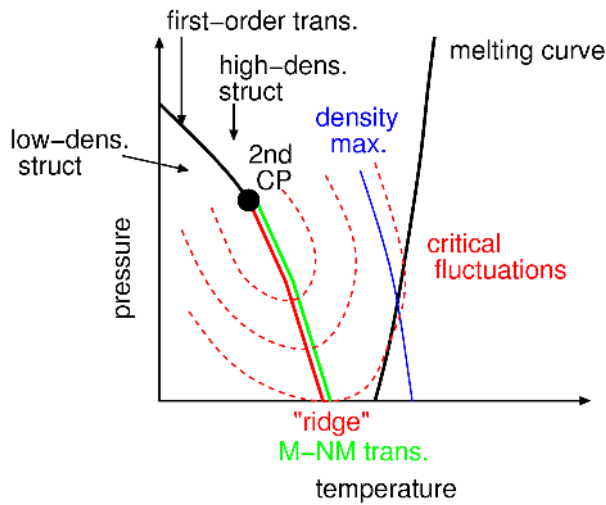
**Figure 7.** (Colour online) Schematic phase diagram of liquid Te. See details in the text.

We introduced the dynamical inhomogeneity, which is defined as the fluctuations with respect to the internal degree of freedom, from the thermodynamic formulation, and explained that when there exists large dynamical inhomogeneity in the system, the positiveness becomes large and the value will be much enhanced at the M-NM transition. The present results should be a direct evidence of the large dynamical inhomogeneity near the melting temperature in liquid Te, which is observed for the first time. Next we considered the reason why there appears large dynamical inhomogeneity in liquid Te. We noticed the similarity of the structural transition in liquid Te and that in liquid water, which reminded us the idea of the second critical fluctuations whose phase diagram has the second critical point. When the second critical fluctuations due to the structural transition which accompany the M-NM transition is assumed, the large dynamical inhomogeneity near the melting point in liquid Te may naturally be understood.

We concluded that IXS technique must be a powerful tool to investigate the second critical fluctuations when the ultrasonic measurements are combined.

### Acknowledgement

### References

[1] Epstein A S, Fritzche H and Lark-Horovitz K 1957 *Phys. Rev.* **107** 412
[2] Cabane B and Friedel J 1971 *J. Phys. (France)* **32** 73
[3] Tourand G and Breil M 1970 *C. R. Acad. Sci. Paris* **B 270** 109
[4] Thurn H and Ruska J 1976 *J. Non-cryst. Solids* **22** 331
[5] Takeda S, Okazaki H and Tamaki S 1985 *J. Phys. Soc. Jpn.* **54** 1890

[6] Gitis M B and Mikhailov I G 1966 *Sov. Phys. Acoust.* **12** 14

[7] Tsuchiya 1991 *J. Phys. Soc. Jpn.* **60** 960

[8] Debenedetti P G 1996 *Metastable Liquids. Concepts and Principles* (Princeton, NJ: Princeton University Press)

[9] Tsuchiya Y and Seymour E F W 1982 *J. Phys.* C **15** L687, 1985 *J. Phys.* C **18** 4721

[10] Johnson V A 1955 *Phys. Rev.* **98** 1567

[11] Rapoport E 1968 *J. Chem. Phys.* **48** 1433

[12] Cohen M H and Jortner J 1976 *Phys. Rev.* B **13** 5255

[13] Endo H, Maruyama K, Hoshino H and Ikemoto H 2003 *Z. Phys. Chem.* **217** 863 and references therein.

[14] Axmann A, Gissler W, Kollmar A and Springer T 1970 *Discuss. Faraday Soc.* **50** 74

[15] Endo H, Tsuzuki T, Yao M, Kawakita Y, Shibata K, Kamiyama T, Misawa M and Suzuki K 1994 *J. Phys. Soc. Jpn.* **63** 3200

[16] Chiba A, Ohmasa Y and Yao M 2003 *J. Chem. Phys.* **119** 9047

[17] Ruiz-Martin M D, Jimenez-Ruiz M, Bermejo F J and Fernandez-Perea R 2006 *Phys. Rev.* B **73** 094201

[18] Hosokawa S, Pilgrim W -C, Demmel F and Albergamo F 2006 *J. Non-Cryst. Solids*, **352** 5114

[19] Kajihara Y, Inui M, Hosokawa S, Matsuda K and Baron A Q R 2008 *J. Phys.: Conf. ser.* **98** 022001

[20] Baron A, Tanaka Y, Miwa D, Ishikawa D, Mochizuki T, Takeshita K, Goto S, Matsushita T, Kimura H, Yamamoto F and Ishikawa T 2001 *Nucl. Instrum. Methods* A **467/468** 627

[21] Tamura K, Inui M and Hosokawa S 1999 *Rev. Sci. Instrum.* **70** 144

[22] Hosokawa S and Pilgrim W -C 2001 *Rev. Sci. Inst.* **72** 1721

[23] Misawa M 1992 *J. Phys.: Condens. Matter* **4** 9491

[24] Barrue R and Perron J C 1985 *Phil. Mag.* B **51** 317

[25] Tsuzuki T, Yao M and Endo H 1995 *J. Phys. Soc. Jpn.* **64** 485

[26] Perron J C 1967 *Adv. Phys.* **16** 657

[27] Litovitz T A and Davis C M 1965 *Physical Acoustics* **IIA** ch 5, ed W P Mason (New York: Academic); Stuehr J and Yeager E *ibid* Ch. 6

[28] In liquid Te, the specific heat ratio is almost 1.0 near the melting temperature and we neglect the difference between the adiabatic and the isothermal compressibility.

[29] We know that the two-state model is too simple in *quantity* to describe the supercritical state which we suggest in the later part of the present paper, but we think it is adequate in *quality* and introduce this model for simplicity.

[30] see eg, Chaikin P M and Lubensky T C 1995 Principles of condensed matter physics (Cambridge university press) Ch. 5.4

[31] Hensel F and Warren W W Jr. 1999 *Fluid Metals* (Princeton Univ Press, Princeton, NJ)

[32] Inui M, Matsuda K, Ishikawa D, Tamura K and Ohishi Y 2007 *Phys. Rev. Lett* **98** 185504

[33] Ishikawa D, Inui M, Matsuda K, Tamura K, Tsutsui S and Baron A Q R 2004 *Phys. Rev. Lett.* **93** 097801

[34] Kohno H and Yao M 2001 *J. Phys.: Condens. Matter* **13** 10293

[35] See review, Debenedetti P G and Stanley H E 2003 *Phys. Today* **56-6** 40

[36] Liu L, Chen S H, Faraone A, Yen C W and Mou C Y 2005 *Phys. Rev. Lett* **95** 117802